

Document downloaded from:

<http://hdl.handle.net/10251/117536>

This paper must be cited as:

Caram, B.; García-Ballesteros, S.; Santos-Juanes Jordá, L.; Arqués Sanz, A.; Garcia-Einschlag, FS. (2018). Humic like substances for the treatment of scarcely soluble pollutants by mild photo-Fenton process. *Chemosphere*. 198:139-146.
<https://doi.org/10.1016/j.chemosphere.2018.01.074>



The final publication is available at

<http://doi.org/10.1016/j.chemosphere.2018.01.074>

Copyright Elsevier

Additional Information

1
2
3
4
5
6
7
8
9
10
11
12
13
14
15
16
17
18
19
20
21
22
23
24
25
26
27
28
29
30
31
32
33
34
35
36
37
38
39
40
41
42
43
44
45
46
47
48
49
50
51
52
53
54
55
56
57
58
59
60
61
62
63
64
65

1 Humic like substances for the treatment of scarcely 2 soluble pollutants by mild photo-Fenton process

3 Bruno Caram¹, Sara García-Ballesteros², Lucas Santos-Juanes^{*2}, Antonio Arques², Fernando S.
4 García-Einschlag¹,

5 1. Instituto de Investigaciones Fisicoquímicas Teóricas y Aplicadas (INIFTA), CCT-La Plata-
6 CONICET, Universidad Nacional de La Plata, Diag 113 y 64, La Plata, Argentina.

7 2. Grupo de Procesos de Oxidación Avanzada, Departamento de Ingeniería Textil y Papelera,
8 Campus de Alcoy, Universitat Politècnica de València. E-03801, Alcoy, Spain.

9 10 ABSTRACT

11 Humic-like substances (HLS) extracted from urban wastes have been tested as auxiliaries for
12 the photo-Fenton removal of thiabendazole (TBZ) under simulated sunlight. Experimental design
13 methodology based on Doehlert matrices was employed to check the effects of hydrogen
14 peroxide concentration, HLS amount as well as TBZ loading; this last parameter was studied in
15 the range 25-100 mg/L, to include values below and above the limit of solubility at pH = 5. Very
16 satisfactory results were reached when TBZ was above solubility if HLS and H₂O₂ amounts were
17 high. This could be attributed to an interaction of HLS-TBZ that enhances the solubility of the

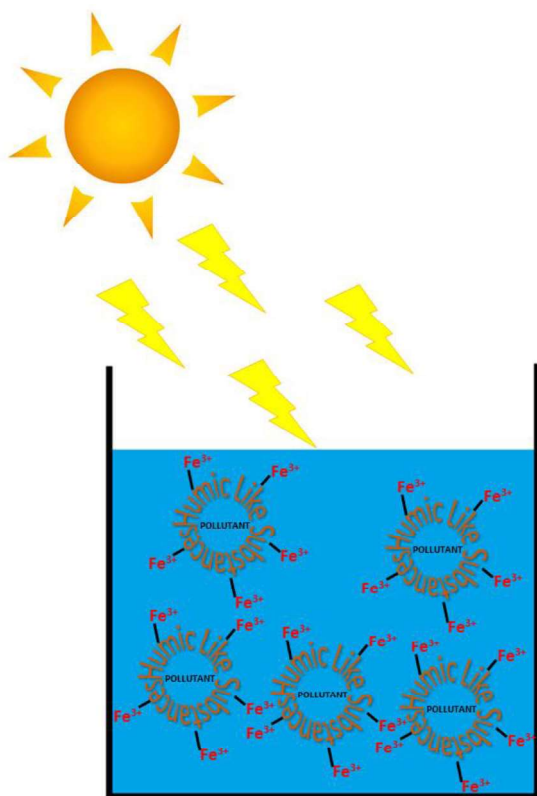
1
2
3
4 18 pollutant. Additional evidence supporting the latter interaction was obtained by fluorescence
5
6
7 19 measurements (excitation emission matrices) and parallel factor analysis (PARAFAC).
8

9 20

10
11 21 **KEYWORDS:** Thiabendazole; photo-Fenton; humic-like substances; EEM; PARAFAC
12
13

14 22

15
16
17 23 **TOC/Abstract Graphic**
18
19



20
21
22
23
24 24

25 **Synopsis:** Humic-like substances extracted from urban wastes enhance photo-Fenton removal
26 of scarcely soluble pollutants under UVA-visible irradiation
27
28
29
30
31
32
33
34
35
36
37
38
39
40
41
42
43
44
45
46
47
48
49
50
51

1
2
3
4 27 1. INTRODUCTION
5
6
7
8 28
9

10 29 The presence of hazardous species in the environment is a serious concern. Compounds such as
11
12 30 pesticides or fungicides can easily accumulate in plants, soil or water bodies because of its
13
14 31 resistance to the action of sunlight or microorganisms. Furthermore, the solubility of many of
15
16 32 these pollutants is low and they are applied in suspensions or emulsions at concentrations above
17
18 33 their solubility limit to ensure its presence in plants or soils during large periods of time (Ibarz et
19
20 34 al. (2016)).
21
22

23
24
25 35 Advanced oxidation processes (AOP) have been successfully explored as a procedure to treat
26
27 36 low soluble pollutants present in soil by combining a washing step with a later oxidation process
28
29 37 (Villa et al. (2010)). One of the most used AOP is the photo-Fenton process, which consists in the
30
31 38 use of iron salts to catalyze the decomposition of hydrogen peroxide into highly reactive species,
32
33 39 such as hydroxyl radical (Pignatello et al. (2006)). The reaction has an optimum pH, namely 2.8,
34
35 40 in order to prevent iron deactivation via formation of hydroxides. Irradiation results in an
36
37 41 acceleration of the photocatalytic process and sunlight can be used for this purpose (Malato et al.
38
39 42 (2009)). However, this acidic pH is a major drawback for large scale applications or 'in situ'
40
41 43 treatments. Hence, research on modified photo-Fenton processes able to work at mild conditions
42
43 44 is meaningful (Santos-Juanes et al. (2017)). One of these strategies involves the use of chemical
44
45 45 auxiliaries to extend the photocatalytic role of iron salts to a milder pH, by forming photoactive
46
47 46 complexes with iron. Carboxylates such as oxalate, EDDS or citric acid have been used for this
48
49 47 purpose with satisfactory results, although in most cases these chemicals are consumed in the
50
51 48 process (Soares et al. (2015), Huang et al. (2012), Klammerth et al. (2012), De Luca et al. (2014)).
52
53
54
55
56
57
58
59
60 49
61
62
63
64
65

1
2
3
4 50 Macromolecules have been employed as chelating agents for photo-Fenton, among them, humic-
5
6
7 51 like substances (HLS). HLS can be obtained from different sources; for instance, soluble
8
9 52 bioorganic substances (SBO) are a group of HLS that can be isolated from urban wastes
10
11 53 following a procedure described elsewhere (Montoneri et al. (2011)). Some experiments have
12
13
14 54 shown that SBO are able to extend the domain of applicability of photo-Fenton to pH values of
15
16 55 ca. 5, with only a slight loss of efficiency which could be considered as acceptable (Gomis et al.
17
18
19 56 (2015a)). Interestingly, recent fluorescence measurements have demonstrated the high ability of
20
21 57 SBO to complex iron at an optimum pH of 5 (García Ballesteros et al. (2017)). In addition to
22
23
24 58 this, SBO have been described to have surface active properties (Negueroles et al. (2017)). The
25
26 59 surfactant behaviour of SBO would result in a double benefit, as in addition to iron complexation
27
28
29 60 to extend photo-Fenton, they might also enable dissolving scarcely soluble pollutants and a pre-
30
31 61 association between the target compound and the catalyst, namely the Fe-SBO complex.
32
33 62 Potential applications for this strategy are rinsing of bottles or surfaces exposed to chemicals
34
35
36 63 (Malato et al. (2000)) or soil remediation (Mulligan et al. (2001)). Substances such as organic
37
38 64 fungicides might be involved in both scenarios as they commonly show low solubility; when
39
40
41 65 fungicides are applied, only partly reach the crops, while an important amount of them can be
42
43 66 found in soils (Reichenberger et al. (2007)). In addition, bottles containing these substances and
44
45
46 67 plastics of greenhouses must be cleaned before disposal, generating a polluted effluent. In this
47
48 68 context, there is some information on the use of photo-Fenton for soil washing effluents
49
50
51 69 containing pesticides (Villa et al. (2010)).

52
53 70

54
55
56 71 With this background, the aim of this work is to investigate the positive role of HLS on photo-
57
58 72 Fenton process, as both chelating agent and solubility enhancer, when treating suspensions of
59
60
61
62
63
64
65

1
2
3
4 73 pollutants at concentrations beyond their limit of solubility. Thiabendazole (TBZ) has been used
5
6
7 74 as model compound, as it is a widely employed broad-spectrum systemic fungicide used in all
8
9 75 kinds of crops, especially fruit and vegetables (Ibarz et al. (2016)). It exhibits moderate-low
10
11 76 solubility in the mild acidic pH domain (Cassens et al. (2013)) what enables performing
12
13
14 77 experiments below and above this value. SBO were the type of HLS chosen, as important
15
16 78 information on their behaviour in photo-Fenton systems at different pH values is available.
17
18
19 79 Experimental design methodology based on Doehlert matrices has been employed to obtain
20
21 80 surface responses, which are useful to study the effect of operational parameters on TBZ
22
23
24 81 degradation.
25

26 82

29 83 2. EXPERIMENTAL SECTION

32 84

35 85 2.1. Reagents

38 86

40 87 TBZ was supplied by Sigma-Aldrich. Its purity was 99% and it was used as received. $\text{FeCl}_3 \cdot 6\text{H}_2\text{O}$
41
42 88 (Panreac) was used as source of iron. Hydrogen peroxide (30% w/w) was also provided by
43
44
45 89 Panreac. Water employed in all solutions was Milli-Q grade.
46

48 90

51 91 The type of SBO employed in this work was CVT230, which was kindly supplied by University
52
53 92 of Turin. Home gardening and park trimming residues (GR) piles aerated for 230 days were used
54
55
56 93 as sourcing materials. The procedure as well as the characterization of the product have been
57
58 94 previously described in detail (Montoneri et al. (2011)). The SBO isolation was performed in a
59
60
61
62
63
64
65

1
2
3
4 95 pilot plant at the Studio Chiono&Associati in Rivarolo Canavese, Italy. It consists in different
5
6
7 96 stages: a) basic digestion of the raw sourcing material, b) elimination of the non-soluble fraction,
8
9 97 c) concentration of the macromolecules also by ultrafiltration and d) drying of the retentate.
10
11 98 CVT230 contains a 38% of carbon and a 4% of nitrogen, with a 72% of volatile solids. Aliphatic
12
13
14 99 chains represent about twice the aromatic structures, carboxylic acids being the most
15
16 100 representative of the functional groups. More details on the physicochemical properties of these
17
18
19 101 substances can be found elsewhere (Gomis et al. 2015b)

20
21
22 102

23 24 103 2.2. Experimental set-up

25
26
27 104
28
29
30 105 Experiments were performed in a cylindrical Pyrex vessel (55 mm i.d.). Irradiations were carried
31
32 106 out with a solar simulator (Sun 2000, ABET Technologies) equipped with a 550 W Xenon Short
33
34
35 107 Arc Lamp; a glass filter was employed to cut off the residual radiation below 300 nm. With this
36
37 108 configuration, the solar simulator had an irradiance of 75 W/m². This value was obtained with an
38
39 109 Acadus 85 radiometer with a response range between 290 and 370 nm.

40
41
42
43 110 For each experiment, the reactor was loaded with 250 mL of solution containing the SBO (in the
44
45 111 range 10-70 mg/L), the pollutant (25-100 mg/L) and iron (5 mg/L). The initial pH was adjusted
46
47
48 112 to the desired value (2.8 or 5.0) by adding diluted sulphuric acid and was left free once the
49
50 113 reaction started. The initial concentration of H₂O₂ was in the range 34-510 mg/L. Samples were
51
52 114 periodically taken for analysis; they were diluted 1.6:0.3 with methanol to ensure complete
53
54
55 115 dissolution of thiabendazole and to prevent further changes in the composition due to the excess
56
57 116 of H₂O₂; then they were filtered through polypropylene (VWR, 0.45 µm).

58
59
60
61
62
63
64
65

1
2
3
4
5
6
7
8
9
10
11
12
13
14
15
16
17
18
19
20
21
22
23
24
25
26
27
28
29
30
31
32
33
34
35
36
37
38
39
40
41
42
43
44
45
46
47
48
49
50
51
52
53
54
55
56
57
58
59
60
61
62
63
64
65

117

118 2.3. Analysis

119

120 The concentration of TBZ was monitored by liquid chromatography. A Perkin Elmer model
121 Flexar UPLC FX-10 was employed, equipped with a reverse phase column (Brownlee Analytical
122 DB-C18). The eluent consisted in an isocratic mixture of acetonitrile (5%) and water (95%) at a
123 0.3 ml/min flow. Detection was based on UV-vis spectrometry at 300 nm.

124 Samples were also analysed by UV-vis spectroscopy, using a UH5300 spectrometer (Hitachi).
125 Spectra were recorded in the 190-500 nm range. Fluorescence emission-excitation matrices were
126 obtained with a modular fluorimeter QuantaMaster (PTI). Samples were excited in the range
127 250-550 nm and emission was recorded in the range 300-600 nm. Before measurements, 2 ml of
128 sample were diluted with 1 ml of methanol and 3 ml of water. pH measurements were performed
129 using a Crison (BASIC 20⁺ model) pH-meter.

130

131 2.4. Experimental design

132

133 To assess the effect of three operational variables (TBZ, SBO and hydrogen peroxide
134 concentrations) an experimental design methodology based on a Doehlert array was used
135 (Ferreira et al. (2004)). A total of 15 experiments (k^2+k+1 , where k is the number of analysed
136 variables, 3 in this study, plus two replicates of the central point) were performed. Being the aim
137 of this work determining the effect of SBO in the treatment of non-soluble substances, the range

1
2
3
4 138 of studied TBZ concentrations should be above and below the limit of solubility for this
5
6
7 139 compound, which was ca. 70-75 mg/L at pH = 5; hence, initial concentrations of 25 mg/L, 62.5
8
9 140 mg/L and 100 mg/L were tested. The concentration of SBO were varied between 10 and 70 mg/L
10
11 141 at seven levels. Finally, hydrogen peroxide was tested at five levels in the range 34 mg/L – 510
12
13 142 mg/L; this range was chosen because of the different amounts of oxidizable organics present in
14
15 143 the experiments: the upper limit was the stoichiometric amount of hydrogen peroxide required to
16
17 144 completely mineralize the highest concentration of TBZ plus an excess of 20%, and the lower
18
19 145 limit was the stoichiometric amount required to oxidize the lowest concentration of TBZ minus a
20
21 146 20%. The initial pH was in all cases 5. Experimental conditions of all experiments can be found
22
23
24
25
26 147 in Table 1.

27
28
29 148
30
31
32
33 149 The irradiation time required to decrease TBZ to 50% of its initial concentration ($t_{50\%}$), obtained
34
35 150 from the plot of the relative TBZ concentration vs. time, or the absolute initial TBZ degradation
36
37 151 rate (calculated from the initial slope of TBZ profile against time) were used as responses. The
38
39 152 software Statgraphics Centurion XVI was used for response surface model fitting by means of
40
41
42 153 the least squares method.

43 44 45 46 154 47 48 49 155 2.5 Analysis of fluorescence datasets

50
51
52 156
53
54
55
56 157 Parallel factor analysis (PARAFAC) (Andersen and Bro (2003)) was used to decompose the sets
57
58 158 of Excitation-Emission-Matrices (EEMs) into independent factors (García-Ballesteros et al.
59
60
61
62
63
64
65

1
2
3
4 159 (2017), Su et al. (2015)). Briefly, given a 3-way array structure containing the EEMs of several
5
6
7 160 samples (\mathbf{X}), the PARAFAC algorithm decomposes \mathbf{X} into three matrices that contain the
8
9 161 relative contribution profiles (A), the normalized emission spectra (B) and the normalized
10
11 162 excitation spectra (C), for each of the factors that compose the observed fluorescent signals. Pre-
12
13
14 163 processing steps, including the correction of inner-filter effects (i.e., primary and secondary),
15
16 164 blank subtraction and the removal of scattering signals (i.e., Rayleigh and Raman), were
17
18
19 165 followed (Ohno (2002), Bahram et al. (2006)). PARAFAC models from two to six factors were
20
21 166 tested. In all cases, non-negativity and unimodality constraints were used to obtain chemically
22
23
24 167 relevant results. The correct number of factors was assessed by the analysis of the physical sense
25
26 168 of spectral loadings as well as the evaluation of the distribution of residuals.

27
28
29 169

30 31 32 33 170 3. RESULTS AND DISCUSSION

34
35 171

36 37 38 172 3.1. Mild photo-Fenton to remove TBZ in the presence of SBO

39
40
41 173

42
43
44 174 A first series of experiments was performed to determine if the presence of SBO was able to
45
46 175 improve the ability of photo-Fenton to remove TBZ. The following experiments were carried
47
48
49 176 out: a) Fe(III) + H₂O₂ at pH = 5 under dark conditions, b) irradiation of TBZ + H₂O₂ at pH = 5,
50
51 177 c) photo-Fenton at pH = 5 without SBO, d) photo-Fenton at pH = 5 with SBO, e) photo-Fenton
52
53
54 178 at pH = 2.8 without SBO, f) photo-Fenton at pH = 2.8 with SBO. The concentration of TBZ was
55
56 179 62.5 mg/L which is a value close to its solubility limit at pH 5 (i.e., 75mg/L); iron concentration
57
58
59 180 was 5 mg/L and, when present, the SBO concentration was 40 mg/L and the initial amount of

1
2
3
4 181 hydrogen peroxide was the stoichiometric amount required to mineralize TBZ, namely 272
5
6
7 182 mg/L. Kinetic profiles can be found in Figure 1; photo-Fenton at pH = 2.8 was always faster than
8
9 183 that at pH = 5; this is not a surprising result, as 2.8 is the optimum pH for photo-Fenton. In fact,
10
11 184 at pH = 5 only photo-Fenton in the presence of SBO could achieve a complete TBZ removal; this
12
13 185 agrees with previous results, which shown that SBO enhanced photo-Fenton at circumneutral pH
14
15 186 by avoiding, via iron complexation, catalyst inactivation (Gomis et al. (2014)). In the same work,
16
17 187 it was reported that SBO may play a detrimental role at pH = 2.8, most probably due to a
18
19 188 competition between SBO and pollutant for the reactive species. However, in experiments here
20
21 189 reported, the effect of SBO was positive even in acidic media: this cannot be attributed to iron
22
23 190 complexation (this is not required at this pH to prevent iron inactivation) and suggests that the
24
25 191 surfactant role of these macromolecules might result in a pre-association of TBZ with the
26
27 192 SBO/Fe system, thus favouring the reaction between the short-lived reactive species and the
28
29 193 pollutant. This effect should be more predominating at higher pollutant concentration, as the
30
31 194 competition of SBO for the active species is not so relevant.
32
33
34
35
36
37
38
39
40

41 195
42 196 In order to gain further insight into the role of SBO in photo-Fenton at pH = 5 and different TBZ
43
44 197 initial amounts, a [TBZ] = 62.5 mg/L was chosen for the central point of the experimental design
45
46 198 because, as stated above, it is close to the solubility limit of this compound. The lowest and the
47
48 199 highest TBZ loadings were 25 and 100 mg/L, with TBZ being completely and partially soluble,
49
50 200 respectively. Both the time required to decrease TBZ to 50% of its initial value ($t_{50\%}$) and the
51
52 201 absolute initial degradation rate (r_{Init}) were used as response parameters.
53
54
55
56
57
58

59 202 It is important to mention that some decrease from the initial pH value of 5 was observed, since
60
61
62
63
64
65

1
2
3
4
5
6
7
8
9
10
11
12
13
14
15
16
17
18
19
20
21
22
23
24
25
26
27
28
29
30
31
32
33
34
35
36
37
38
39
40
41
42
43
44
45
46
47
48
49
50
51
52
53
54
55
56
57
58
59
60
61
62
63
64
65

204 values slightly below 4 were recorded at the end of the process. This is a very well-known
205 behaviour due to the release of carboxylic intermediates. However, this change was slow enough
206 to have negligible effect on the kinetics at the early stages of the reaction.

207
208 Despite the experimental problems associated with the use TBZ loadings above the solubility
209 limit, the regression coefficient was reasonable (91.4%). Pareto chart (see supplementary
210 material, FS1), show that concentration of hydrogen peroxide and SBO were the most significant
211 parameters. The response surface describing $t_{50\%}$ values is given by Equation 1

$$t_{50\%} = 37.7 - 0.24 \cdot [H_2O_2] - 0.21 \cdot [SBO] + 1.34 \cdot [TBZ] + 0.00034 \cdot [H_2O_2]^2 + 0.00007 \cdot [H_2O_2] \cdot [SBO] - 0.00030 \cdot [H_2O_2] \cdot [TBZ] + 0.0024 \cdot [SBO]^2 - 0.0056 \cdot [SBO] \cdot [TBZ] - 0.0071 \cdot [TBZ]^2$$

(Equation 1)

217
218 Despite valuable information can be extracted from the analysis of coefficients of Equation 1, it
219 is difficult to visualize the effect of each parameter in the three-dimensional domain described by
220 this response surface. For this reason, different bi-dimensional functions were obtained by fixing
221 one parameter at a given value, since they can be represented by contour plots. Figure 2 shows
222 plots obtained by using the coefficients of Equation 1 and fixing each parameter at three levels:
223 high, central and low value.

224
225 Plots obtained when fixing [SBO] at high, low and central levels (65, 40 and 15 mg/L

1
2
3
4 226 respectively) followed similar patterns: the $t_{50\%}$ value was mostly ruled by the concentration of
5
6
7 227 peroxide below 150-250 mg/L. Above this point, $t_{50\%}$ became nearly independent of H_2O_2 ,
8
9 228 although a certain loss of efficiency can be appreciated at the highest oxidant concentrations; the
10
11 229 detrimental effect of an excess of H_2O_2 has been reported elsewhere and it is attributable to
12
13
14 230 scavenging of the reactive species, namely $\bullet OH$ (Santos-Juanes et al. (2011)). Finally, it can be
15
16 231 observed that TBZ loading has only a minor effect at high concentrations of SBO, while for low
17
18
19 232 amounts of added SBO, an increase in TBZ loading results in a higher $t_{50\%}$, and hence, a loss of
20
21 233 efficiency. This seems a first hint that SBO plays a favourable role by enhancing TBZ solubility.
22
23

24 234
25
26
27 235 The initial loading of TBZ was also fixed at three points (90, 62.5, and 35 mg/L). The effect of
28
29 236 H_2O_2 was also clear in this case, with optimal values in the range 300-400 mg/L. However, very
30
31
32 237 important differences in the plots can be appreciated regarding to the effect of SBO
33
34 238 concentration. For the lowest TBZ amount, the contour lines are predominantly vertical, showing
35
36
37 239 that the effect of $[H_2O_2]$ is much more important than that of $[SBO]$; however, as TBZ loading
38
39 240 approaches to the solubility limit, contour lines become more oblique, showing an increase of the
40
41 241 importance of the $[SBO]$; this agrees with this macromolecule playing a surfactant role, hence
42
43
44 242 favouring the contact between the reactive species and the pollutant.
45
46

47 243
48
49
50 244 The same procedure was followed with the concentration of hydrogen peroxide. Very similar
51
52 245 values of $t_{50\%}$ were obtained at the central and high levels (272 and 450 mg/L) while treatment
53
54 246 efficiencies significantly decrease at the lowest level (100 mg/L), indicating that a certain
55
56
57 247 amount of hydrogen peroxide is required for achieving important conversion degrees within the
58
59 248 first hour of treatment. Interestingly, in all three scenarios the worst performance was reached at
60
61
62
63
64
65

1
2
3
4 249 high pollutant loadings and low [SBO], indicating that close or above TBZ solubility the
5
6
7 250 presence of SBO is required for an efficient treatment, in agreement with previous observations.
8

9 251
10
11
12 252 A response surface was also obtained (equation 2) from the absolute initial reaction rates (r_{init} ,
13
14 253 given as mg converted per minute and litter) of TBZ removal (data shown in Table 1). The
15
16
17 254 regression coefficient was also good (93.7%) and Pareto chart (see supplementary material, FS1)
18
19 255 shows that in this case all three parameters became significant, as well as the interaction between
20
21
22 256 the concentrations of SBO and TBZ. Data based on r_{init} can provide complementary information
23
24 257 to $t_{50\%}$, as the time required to decrease the initial concentration in a 50% is a relative value that
25
26
27 258 characterizes the overall transformation rate while the initial rate is an absolute parameter
28
29 259 describing the system behaviour at the beginning of the treatment.
30
31

32 260
33
34
35 261 $r_{init} \text{ (mg L}^{-1} \cdot \text{min}^{-1}) = 1.13 + 0.967 \cdot 10^{-3} \cdot [\text{H}_2\text{O}_2] - 27.4 \cdot 10^{-3} \cdot [\text{SBO}] - 21.7 \cdot 10^{-3} \cdot [\text{TBZ}] - 3.02 \cdot 10^{-6} \cdot [\text{H}_2\text{O}_2]^2 + 47.3 \cdot 10^{-6} \cdot [\text{H}_2\text{O}_2] \cdot [\text{SBO}] - 9.62 \cdot 10^{-6} \cdot [\text{H}_2\text{O}_2] \cdot [\text{TBZ}] - 6.94 \cdot 10^{-6} \cdot [\text{SBO}]^2 + 0.498 \cdot 10^{-3} \cdot [\text{SBO}] \cdot [\text{TBZ}] + 0.086 \cdot 10^{-3} \cdot [\text{TBZ}]^2$
36
37 262
38
39 263
40
41

42 264 (Equation 2)
43
44

45 265
46
47
48 266 As done with $t_{50\%}$, contour plots were obtained by fixing each parameter at three different levels
49
50 267 (Figure 3). When fixing [SBO], it can be appreciated that at the highest level, the r_{init} increases
51
52
53 268 with the amount of TBZ if there is enough availability of hydrogen peroxide. In fact, the plot
54
55 269 shows values ranging from below 0.3 mg/(L·min) to above 3 mg/(L·min). The same behaviour is
56
57
58 270 observed at the central [SBO] although variation in r_{init} is not so remarkable (values in the range
59
60 271 0.3-1.8 mg/(L·min)). On the contrary, for the low [SBO] no significant variation of r_{init} in the
61
62
63
64
65

1
2
3
4 272 experimental region was observed. When fixing TBZ loading at the highest level, a clear positive
5
6
7 273 effect of SBO can be appreciated, as reaction rate increases with the concentration of this
8
9 274 macromolecule; this effect is observed to a minor extent at the central TBZ value and it is
10
11 275 practically not found for TBZ fixed at the lowest loading, clearly below the solubility of this
12
13
14 276 compound. Finally, when fixing hydrogen peroxide at the three levels, a strong interaction
15
16 277 between the amounts of TBZ and SBO was observed in all cases, as the reaction was faster in the
17
18
19 278 region where the levels of both, SBO and TBZ, were high.

20
21 279
22
23
24 280 Putting all results together, it can be stated that SBO has a positive role on the decomposition of
25
26
27 281 TBZ when the loading of this pollutant is close or above its limit of solubility, while it is not so
28
29 282 evident at lower amounts of TBZ; this is more clearly appreciated when analysing r_{init} than $t_{50\%}$.
30
31 283 Furthermore, it can be appreciated that, for high TBZ loadings, increasing [SBO] results in an
32
33
34 284 enhancement of the reaction rates. This is a different behaviour from that reported for other
35
36 285 pollutants (pesticides and pharmaceuticals) at concentrations of 5 mg/L (Gomis et al. (2015)),
37
38
39 286 where an optimal SBO concentration was observed and beyond this point, further addition of this
40
41 287 substance was detrimental. This was attributed to competition of SBO with the pollutant for the
42
43
44 288 reactive species and the inner filter effect exerted by this coloured substance, which became
45
46 289 more important than the enhancement in reactive species generation associated with the iron-
47
48
49 290 complexing ability of SBO. However, when pollutants are close to their solubility limit, an extra
50
51 291 factor must be considered, namely the ability of SBO to act as surfactant, which favours the
52
53
54 292 contact between the reactive species and TBZ in solution.

55
56 293
57
58
59 294 3.2. Mechanistic studies
60
61
62
63
64
65

1
2
3
4 295
5
6
7 296 As the positive role of SBO in the degradation of TBZ in photo-Fenton systems should be
8
9 297 attributed to a kind of interaction between the pollutant and the humic-like substance, devoting
10
11 298 further research to investigate of the nature of this interaction seems interesting. Since UV-vis
12
13 299 spectra did not provide clear evidence of TBZ-SBO interaction, fluorescence measurements were
14
15 300 performed. The excitation-emission matrices (EEM) were recorded in solutions containing 20
16
17 301 mg/L of TBZ at increasing concentrations of SBO (0, 25, 50, 75 and 100 mg/L) at pH=5. EEM
18
19 302 are bi-dimensional plots showing the emission of fluorescence at a given wavelength upon
20
21 303 excitation at another wavelength (García Ballesteros et al. (2017), Ohno (2002), Bahram et al.
22
23 304 (2006), Ohno et al. (2008)); the obtained EEM can be observed in Figure 4.
24
25
26
27
28
29
30
31

305
32 306 In order to gain further insight into the composition of the system under the studied conditions, a
33
34 307 PARAFAC analysis was performed. This is a mathematical procedure commonly employed to
35
36 308 study complex mixtures, which allows determining the number of fluorescent contributions as
37
38 309 well as their spectral features. In this case, the aim of this analysis was to obtain valuable
39
40 310 information that supported the interaction between the SBO and the model pollutant. PARAFAC
41
42 311 analysis of EEMs shown in Figure 5 indicated that the experimental data could be adequately
43
44 312 fitted to a model consisting in 5 components, the emission and excitation spectra of which can be
45
46 313 seen in Figure 5. Two of these components, with emission maxima at 344 nm and 350 nm, were
47
48 314 also observed for TBZ solutions free of BOS and may be ascribed to the acidic (F1) and neutral
49
50 315 (F3) forms of TBZ, respectively. Other two factors (whose emission maxima are at 444 and 532
51
52 316 nm) could be assigned to SBO (F4 and F5), according to previous studies performed with these
53
54 317 substances (García Ballesteros et al. (2017)). Interestingly, a fifth factor (F2) was found, whose
55
56
57
58
59
60
61
62
63
64
65

1
2
3
4 318 emission maximum was close to 360 nm; this component can solely be observed for solutions
5
6
7 319 where both TBZ and SBO were present, and hence it should be assigned to an interaction TBZ-
8
9 320 SBO. Noteworthy, the contribution of this latter factor increases with increasing [SBO].

10
11
12 321
13
14
15 322 Additional tests were performed to characterize the fluorescent behaviour of acid and neutral
16
17 323 forms of TBZ. In this context, EEM were recorded for TBZ solutions of different pH in the
18
19 324 absence of SBO (Figure SF3, Supporting Information). PARAFAC analysis yielded two main
20
21
22 325 factors, corresponding to acidic and neutral forms of TBZ. Interestingly, a third contribution
23
24 326 appeared and it was observed to increase at pH above 4.5. This value is close to the pK_a of TBZ
25
26
27 327 (4.8 according to the literature (Cassens et al. 2013)), in coincidence with the predominance of
28
29 328 neutral form of TBZ, which is less soluble than the corresponding acidic form. Furthermore, the
30
31
32 329 first order Rayleigh dispersion band increased, which is commonly observed in the presence of
33
34 330 suspended material in the sample (Ohno et al. (2008)). Hence, this third contribution could be
35
36
37 331 associated with the formation of aggregates of the neutral form of TBZ, due to its
38
39 332 hydrophobicity. It is important to remark that in the presence of SBO and at pH = 5, the EEM
40
41
42 333 analysed showed no evidence of aggregates, thus providing an additional piece of evidence of
43
44 334 the interaction TBZ-SBO, which prevents precipitation of the pesticide.

45
46
47 335
48
49 336 4. CONCLUSIONS

50
51
52 337
53
54
55 338 Humic-like substances have been demonstrated as interesting additives for the removal of
56
57 339 scarcely soluble pollutants, close or above their limits of solubility, via photo-Fenton processes.
58
59
60 340 This result is interesting in view of applying a procedure that involves combination of soil
61
62
63
64
65

1
2
3
4 341 washing with the SBO, followed by a solar photo-Fenton to treat the obtained effluent. Hence,
5
6
7 342 further research in this field is meaningful, namely with simulated or real soils polluted with the
8
9 343 pesticide.

10
11
12 344
13
14
15 345 Photophysical studies, based on the analysis of EEM-datasets by the PARAFAC algorithm, have
16
17 346 shown the existence of an interaction between the SBO and the model pollutant. This
18
19
20 347 methodology has appeared as especially interesting to unveil mechanistic aspects of photo-
21
22 348 oxidative processes when dealing with complex mixtures.

23
24
25 349

26
27 350 AUTHOR INFORMATION

28
29
30 351 **Corresponding Author**

31
32
33 352 *lusanju1@txp.upv.es

34
35
36
37 353 The manuscript was written through contributions of all authors. All authors have given approval
38
39 354 to the final version of the manuscript. All authors contributed equally.

40
41
42
43 355

44
45
46 356

47
48
49 357 ACKNOWLEDGMENTS

50
51
52 358 Authors want to acknowledge the financial support of Spanish Ministerio de Economía y
53
54 359 Competitividad (CTQ2015-69832-C04) and European Union (645551-RISE-2014,
55
56 360 MAT4TREAT). The present work was partially supported by UNLP (11/X679) and CONICET

57
58
59
60
61
62
63
64
65

1
2
3
4
5
6
7
8
9
10
11
12
13
14
15
16
17
18
19
20
21
22
23
24
25
26
27
28
29
30
31
32
33
34
35
36
37
38
39
40
41
42
43
44
45
46
47
48
49
50
51
52
53
54
55
56
57
58
59
60
61
62
63
64
65

361 (PIP: 12-2013-01-00236CO). B. Caram thank the CONICET for his research graduate grant. F.
362 S. García Einschlag is a research member of CONICET

364 REFERENCES

365 Andersen, C. M., Bro, R., 2003. Practical aspects of PARAFAC modeling of fluorescence
366 excitation-emission data. *Journal of Chemometrics* 17, 200-215.

367 Bahram, M., Bro, R., Stedmon, C., Afkhami, A., 2006. Handling of Rayleigh and Raman scatter
368 for PARAFAC modeling of fluorescence data using interpolation. *Journal of Chemometrics* 20
369 (3-4), 99-105.

370 Cassens, J., Prudic, A., Ruether, F., Sadowski, G., 2013. Solubility of Pharmaceuticals and Their
371 Salts As a Function of pH. *Industrial and Engineering Chemistry Research* 52, 2721-2731.

372 Chlou, C.T., Malcolm, R.L., Brinton, T.I., Kille, D.E., 1986. Water Solubility Enhancement of
373 Some Organic Pollutants and Pesticides by Dissolved Humic and Fulvic Acids. *Environmental
374 Science and Technology* 20, 502-508.

375 De Luca, A., Dantas, R.F., Esplugas, S., 2014. Assessment of iron chelates efficiency for photo-
376 Fenton at neutral pH. *Water Research* 61, 232-242.

377 Ferreira, S.L.C., dos Santos, W.N.L., Quintella, C.M., Neto, B.B., Bosque-Sendra, J.M., 2004.
378 Doehlert matrix: a chemometric tool for analytical chemistry-review. *Talanta* 63, 1061-1067.

379 García Ballesteros, S., Constante, M., Vicente, R., Mora, M., Amat, A.M., Arques, A., Carlos,
380 L., García Einschlag, F. S., 2017. Humic-like substances from urban waste as auxiliaries for
381 photo-Fenton treatment: a fluorescence EEM-PARAFAC study. *Photochemical and
382 Photobiological Sciences* 16, 38–45.

1
2
3
4 383 Gomis, J., Bianco Prevot, A., Montoneri, E., González, M.C., Amat, A.M., Mártire, D.O.,
5
6
7 384 Arques, A., Carlos, L., 2014. Waste sourced bio-based substances for solar-driven wastewater
8
9 385 remediation: Photodegradation of emerging pollutants. *Chemical Engineering Journal* 235, 236-
10
11 386 243.
12
13
14 387 Gomis, J., Carlos, L., Bianco Prevot, A., Teixeira, A.C.S.C., Mora, M., Amat, A.M., Vicente, R.,
15
16 388 Arques, A., 2015b. Bio-based substances from urban waste as auxiliaries for solar photo-Fenton
17
18 389 treatment under mild conditions: optimization of operational variables. *Catalysis Today* 240, 39-
19
20
21 390 45.
22
23
24 391 Gomis, J.; Gonçalves, M.G.; Vercher, R.F.; Sabater, C.; Castillo, M.A.; Bianco Prevot, A.;
25
26 392 Amat, A. M.; Arques, A, 2015d. Determination of photostability, biocompatibility and efficiency
27
28 393 as photo-Fenton auxiliaries of three different types of soluble bio-based substances (SBO). *Catal.*
29
30
31 394 *Today*, 252, 177–183. Huang, W., Brigante, M., Wu, F., Hanna, K., Mailhot, G. 2012.
32
33 395 Development of a new homogenous photo-Fenton process using Fe(III)-EDDS complexes.
34
35
36 396 *Journal of Photochemistry and Photobiology A: Chemistry*, 239, 17-23.
37
38 397 Ibarz, R., Garvín, A., Aguilar, K., Ibarz, A., 2016. Kinetic study and modelling of the UV photo-
39
40
41 398 degradation of thiabendazole. *Food Research International* 81, 133-140.
42
43 399 Klamerth, N., Malato, S., Aguera, A., Fernandez-Alba, A., Mailhot, G. 2012. Treatment of
44
45
46 400 municipal wastewater treatment plant effluents with modified photo-fenton as a tertiary
47
48 401 treatment for the degradation of micro pollutants and disinfection. *Environmental Science and*
49
50
51 402 *Technology* 46 (5), 2885-2892.
52
53 403 Malato, S., Blanco, J., Richter, C., Maldonado, M.I., 2000. Optimization of pre-industrial solar
54
55 404 photocatalytic mineralization of commercial pesticides: Application to pesticide container
56
57
58 405 recycling. *Applied Catalysis B: Environmental* 25, 31-38.
59
60
61
62
63
64
65

1
2
3
4 406 Malato, S., Fernández-Ibañez, P., Maldonado, M.I., Blanco, J., Gernjak, W., 2009.
5
6
7 407 Decontamination and disinfection of water by solar photocatalysis: Recent overview and trends.
8
9 408 Catalysis Today 147, 1-59.
10
11 409 Montoneri, E., Boffa, V., Savarino, P., Perrone, D.G., Ghezzi, M., Montoneri, C., Mendichi, M.,
12
13
14 410 2011. Acid soluble bio-organic substances isolated from urban bio-waste. Chemical composition
15
16 411 and properties of products. Waste Management 31, 10-17.
17
18
19 412 Montoneri, E., Mainero, D., Boffa, V., Perrone, D.G., Montoneri, C., 2011. Biochemenergy: a
20
21 413 project to turn an urban wastes treatment plant into biorefinery for the production of energy,
22
23
24 414 chemicals and consumer's products with friendly environmental impact. International Journal of
25
26 415 Global Environmental Issues 11, 170-196.
27
28
29 416 Mulligan, C.N., Yong, R.N., Gibbs, B.F., 2001. Surfactant-enhanced remediation of
30
31 417 contaminated soil: a review. Engineering Geology 60, 371-380.
32
33
34 418 Negueroles, P.G., Bou-Belda, E., Santos-Juanes, L., Amat, A., Arques, A., Vercher, R. F.,
35
36 419 Monllor, P., Vicente, R., 2017. Treatment and reuse of textile wastewaters by mild solar photo-
37
38 420 Fenton in the presence of humic-like substances. Environmental Science And Pollution Research
39
40
41 421 24, 12664-12672.
42
43 422 Ohno, T., 2002. Fluorescence Inner-Filtering Correction for Determining the Humification Index
44
45
46 423 of Dissolved Organic Matter. Environmental Science and Technology 36, 742-746.
47
48 424 Ohno, T., Amirbahman, A., Bro, B., 2008. Parallel factor analysis of excitation–emission matrix
49
50
51 425 fluorescence spectra of water soluble soil organic matter as basis for the determination of
52
53 426 conditional metal binding parameters. Environmental Science and Technology 42, 186-192.
54
55
56
57
58
59
60
61
62
63
64
65

1
2
3
4 427 Pignatello, J.J., Oliveros, E., MacKay A., 2006. Advanced oxidation processes for organic
5
6
7 428 contaminant destruction based on the Fenton reaction and related chemistry. *Critical Reviews in*
8
9 429 *Environmental Science and Technology* 36, 1-84.
10
11 430 Reichenberger, S., Bach, M., Skitschak, A., Frede, H.G., 2007. Mitigation strategies to reduce
12
13
14 431 pesticide inputs into ground- and surface water and their effectiveness; A review. *Science of the*
15
16 432 *Total Environment* 384, 1-35.
17
18
19 433 Santos-Juanes, L., Sánchez, J.L.G., López, J.L.C., Oller, I., Malato, S., Sánchez Pérez, J.A.,
20
21 434 2011. Dissolved oxygen concentration: A key parameter in monitoring the photo-Fenton process.
22
23
24 435 *Applied Catalysis B: Environmental* 104, 316-323.
25
26 436 Santos-Juanes, L., Amat, A.M., Arques, A., 2017. Strategies to Drive Photo-Fenton Process at
27
28
29 437 Mild Conditions for the Removal of Xenobiotics from Aqueous Systems. *Current Organic*
30
31 438 *Chemistry* 21, 1074-1083.
32
33
34 439 Soares, P.A., Batalha, M., Souza, S.M.A.G.U., Boaventura, R.A.R., Vilar, V.J.P., 2015.
35
36 440 Enhancement of a solar photo-Fenton reaction with ferric-organic ligands for the treatment of
37
38 441 acrylic-textile dyeing wastewater. *Journal of Environmental Management* 152, 120-131.
39
40
41 442 Su, Y., Chen, F., Liu, Z., 2015. Comparison of optical properties of chromophoric dissolved
42
43 443 organic matter (CDOM) in alpine lakes above or below the tree line: insights into sources of
44
45
46 444 DOM. *Photochemical and Photobiological Sciences* 14, 1047-1062.
47
48 445 Villa, R.D., Trovó, A.G., Nogueira, R.F.P., 2010. Soil remediation using a coupled process: soil
49
50 446 washing with surfactant followed by photo-Fenton oxidation. *Journal of Hazardous Materials*
51
52
53 447 174, 770–775.
54
55
56
57
58
59
60
61
62
63
64
65

1
2
3
4
5
6
7
8
9
10
11
12
13
14
15
16
17
18
19
20
21
22
23
24
25
26
27
28
29
30
31
32
33
34
35
36
37
38
39
40
41
42
43
44
45
46
47
48
49
50
51
52
53
54
55
56
57
58
59
60
61
62
63
64
65

448 Vione, D., Minella, M., Maurino, V., Minero, C., 2014. Indirect photochemistry in sunlight
449 surface waters: photoinduced production of reactive transient species. Chemical European
450 Journal 20, 10590-10606.

451

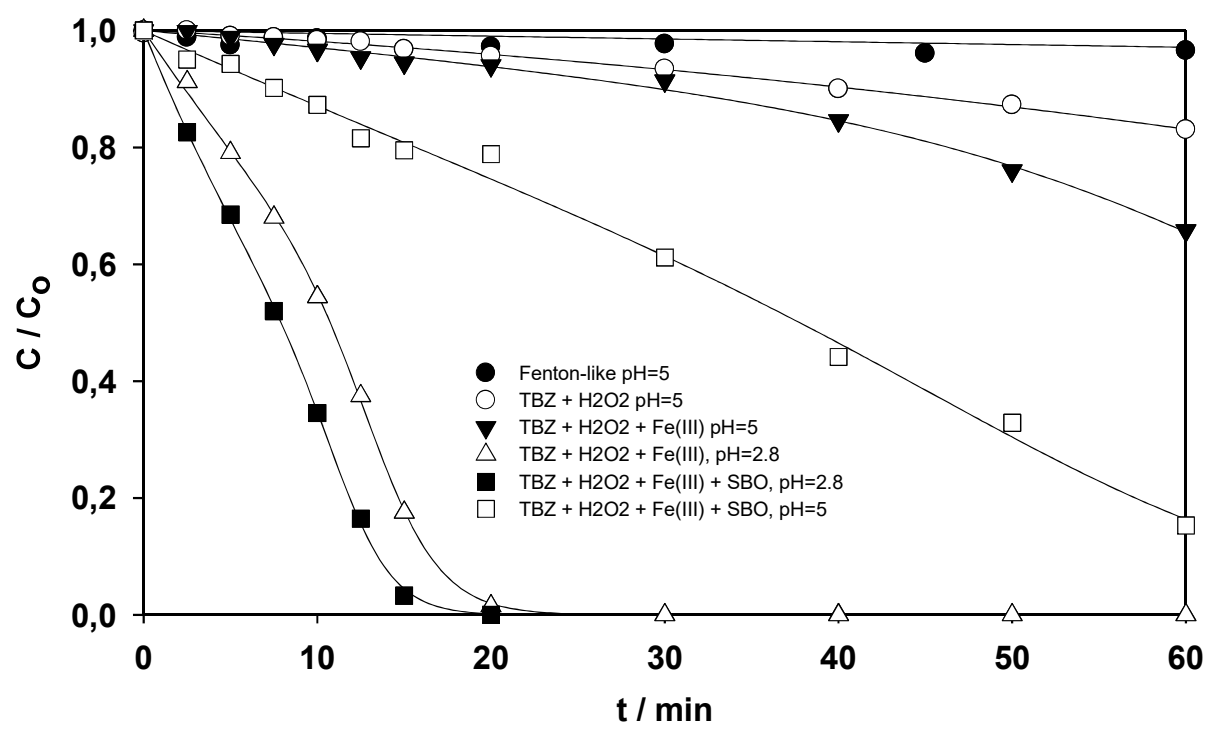
1
2
3
4 452 **Table 1:** Experimental points used to obtain the response surface (Doehlert matrix). The
5
6 453 concentrations of H₂O₂, TBZ and SBO are expressed as mg/L⁻¹. Data given in the last two
7
8
9 454 columns correspond to a) the time (in min) required to decrease concentration of each EP to 50%
10
11 455 of the initial value, and b) the initial reaction rate for the same reaction.
12
13

Coded values			Uncoded Values			Responses	
X ₁	X ₂	X ₃	[H ₂ O ₂] (mg/L)	[SBO] (mg/L)	[TBZ] (mg/L)	t _{50%} (min)	r _{Ini} (mg/(L·min))
0	0	0	272	40	62.5	37	0.863
1	0	0	510	40	62.5	28	1.225
0.5	0.866	0	391	70	62.5	21	1.644
0.5	0.289	0.817	391	50	100	22	2.300
-1	0	0	34	40	62.5	76	0.375
-0.5	-0.866	0.000	153	10	62.5	56	0.538
-0.5	-0.289	-0.817	153	30	25	24	0.370
0.5	-0.866	0.000	391	10	62.5	44	0.581
0.5	-0.289	-0.817	391	30	25	19	0.673
-0.5	0.866	0	153	70	62.5	32	0.925
0	0.577	-0.817	272	60	25	16	0.833
-0.5	0.289	0.817	153	50	100	32	1.600
0	-0.577	0.817	272	20	100	37	0.600
0	0	0	272	40	62.5	26	1.094
0	0	0	272	40	62.5	31	0.956

14
15
16
17
18
19
20
21
22
23
24
25
26
27
28
29
30
31
32
33
34
35
36
37
38
39
40
41
42
43
44
45
46
47
48
49
50
51 456
52
53
54
55
56
57
58
59
60
61
62
63
64
65

1
2
3
4
5
6
7
8
9
10
11
12
13
14
15
16
17
18
19
20
21
22
23
24
25
26
27
28
29
30
31
32
33
34
35
36
37
38
39
40
41
42
43
44
45
46
47
48
49
50
51
52
53
54
55
56
57
58
59
60
61
62
63
64
65

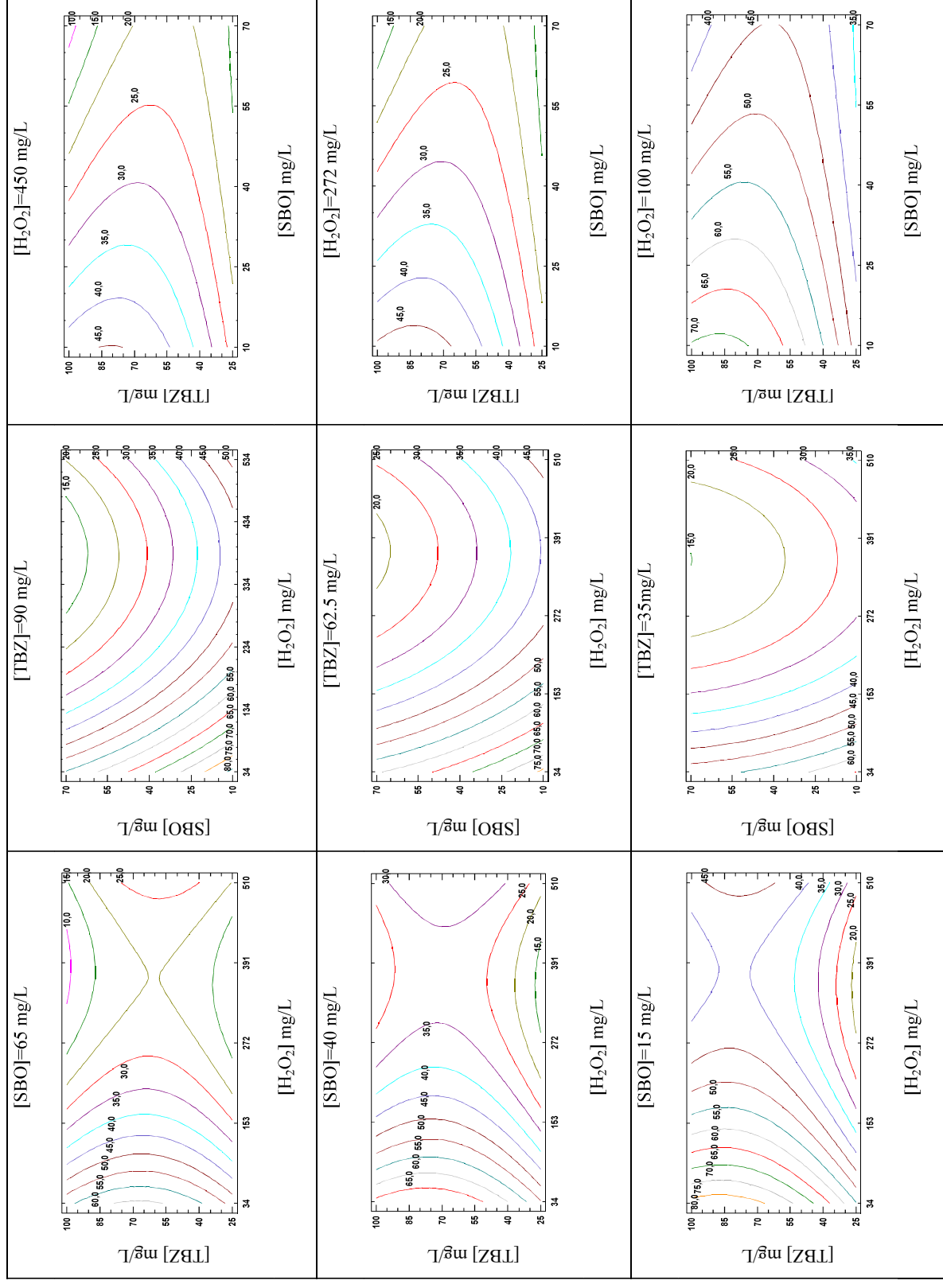
457 **Figure 1:** Plot of the relative concentration of TBZ vs irradiation time under the following
458 experimental conditions $[TBZ]_0 = 62.5$ mg/L, $[H_2O_2] = 272$ mg/L, when was present, $[Fe(III)] =$
459 5 mg/L and $[SBO] = 40$ mg/, (●) dark Fenton at pH = 5, (○) TBZ + H₂O₂ at pH = 5, (Δ) photo-
460 Fenton at pH = 2.8, (■) photo-Fenton with SBO at pH = 2.8, (▼) photo-Fenton at pH = 5, (□)
461 photo-Fenton with SBO at pH = 5



462
463

1
2
3
4
5
6
7
8
9
10
11
12
13
14
15
16
17
18
19
20
21
22
23
24
25
26
27
28
29
30
31
32
33
34
35
36
37
38
39
40
41
42
43
44
45
46
47
48
49

Figure 2. Contour plots for $t_{50\%}$ values obtained from Equation 1 at selected values of each studied parameter



4672
3
4
5
6
7
8
9
10
11
12
13
14
15
16
17
18
19
20
21
22
23
24
25
26
27
28
29
30
31
32
33
34
35
36
37
38
39
40
41
42
43
44
45
46
47
48
49

Figure 3. Contour plots for r_{init} values obtained from Equation 2 at selected values of each studied parameter

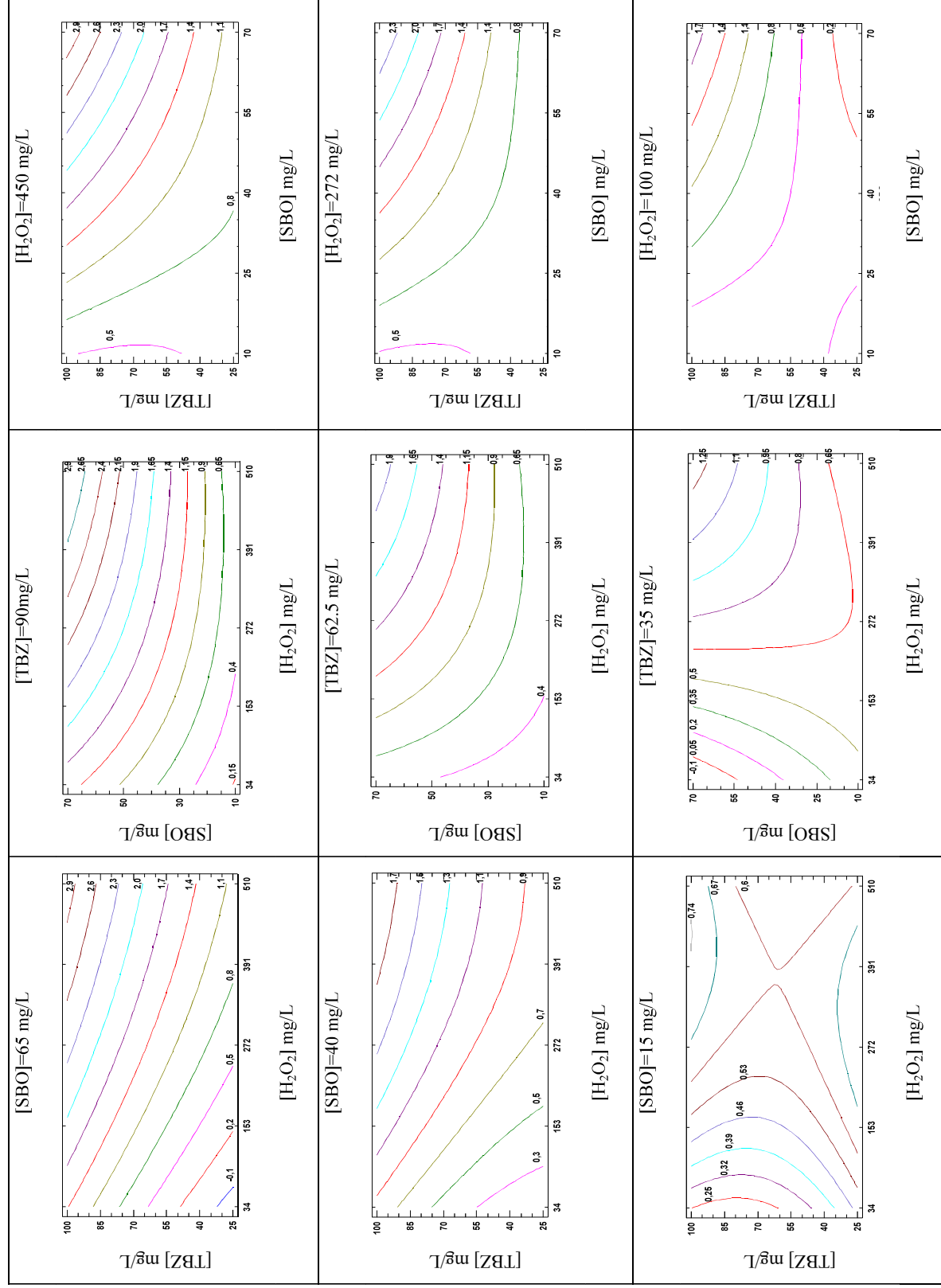
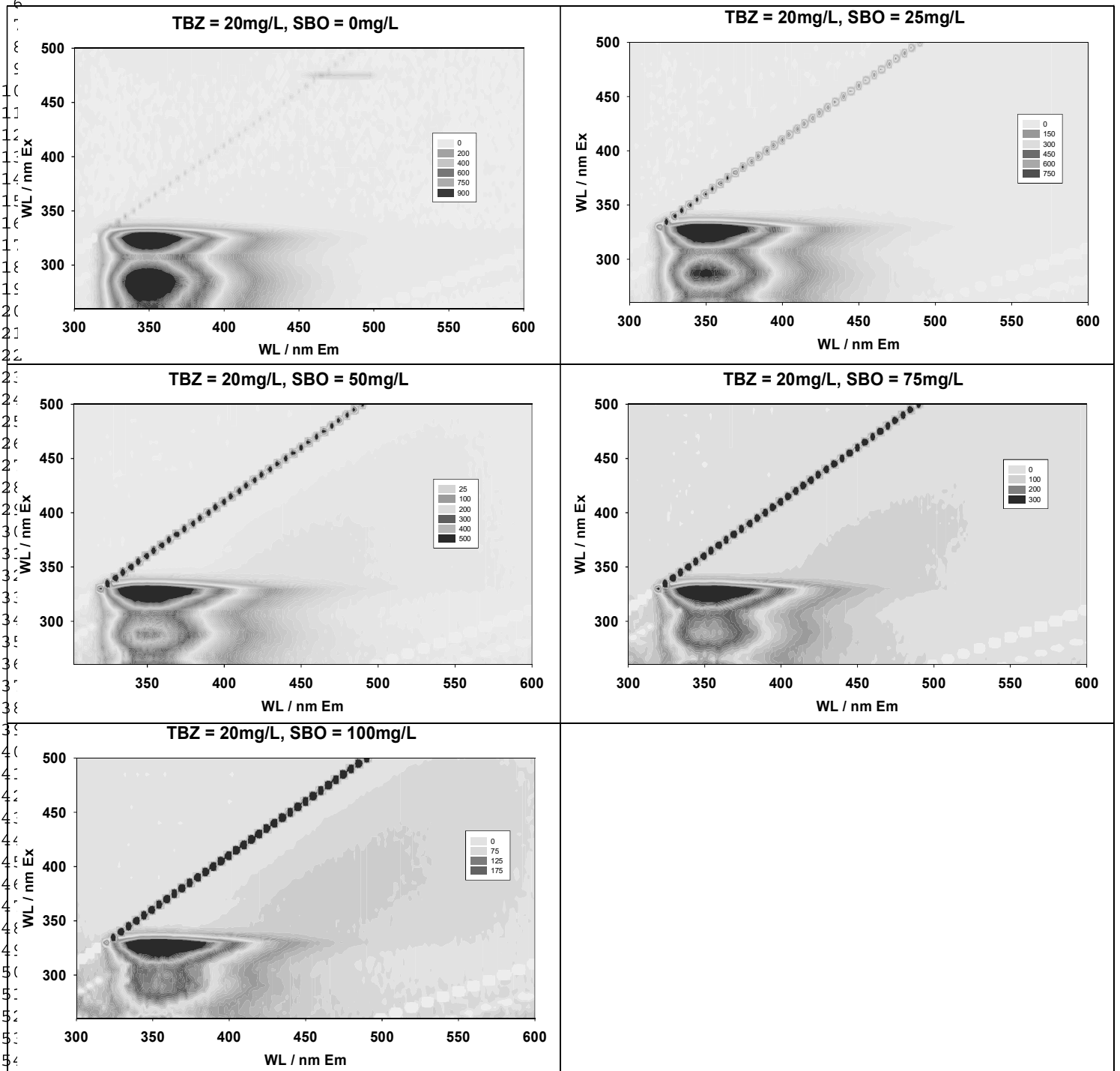
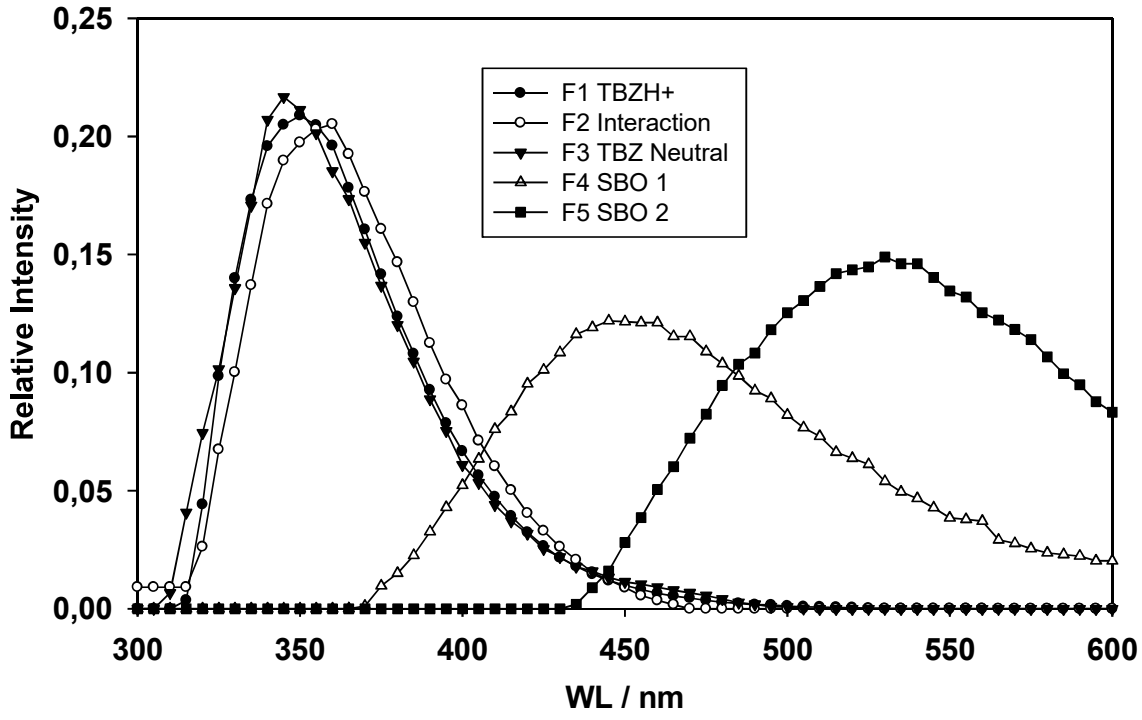


Figure 4. Absorbance corrected EEM obtained for TBZ solutions in the presence of increasing SBO concentrations.



1
2
3
4 **Figure 5.** Emission spectra obtained by PARAFAC decomposition of EEM datasets recorded for TBZ aqueous solution
5
6 containing different concentrations of SBO.
7
8
9
10



37
38
39
40
41
42
43
44
45
46
47
48
49
50
51
52
53
54
55
56
57
58
59
60
61
62
63
64
65